Supplementary Information

Carbohydrate binding through first- and second-sphere coordination within aromatic oligoamide metallofoldamers

Pedro Mateus,[a] Barbara Wicher,[b] Yann Ferrand*[a] and Ivan Huc*[a,c] ¶

[a] *Univ. Bordeaux and CNRS, CBMN (UMR 5248), IECB, 2 rue Robert Escarpit, F-33600 Pessac, France.*
[b] *Department of Chemical Technology of Drugs, Poznan University of Medical Sciences, Grunwaldzka 6, 60-780 Poznan, Poland.*
c.Department of Pharmacy, Ludwig-Maximilians-Universität, Butenandtstraße 5-13, D-81377 München. Germany
E-mail: y.ferrand@cbmn.u-bordeaux.fr, ivan.huc@cup.lmu.de.

This PDF file includes:

1 Materials and Methods for chemical synthesis

All reactions were carried out under a dry nitrogen atmosphere. Commercial reagents were purchased from Sigma-Aldrich, Alfa-Aesar or TCI and were used without further purification unless otherwise specified. Oligomer **1** was obtained as described before.[1] Chloroform ($CHCl_3$) and diisopropylethylamine (DIEA) were distilled over calcium hydride (CaH_2) prior to use. Reactions were monitored by thin layer chromatography (TLC) on Merck silica gel 60-F254 plates and observed under UV light. GPC purification was performed on an LC-9130G NEXT setup (Japan Analytical Industry Co., Ltd.) equipped with two preparative columns (Inner diameter of 20mm and length of 600mm): a JAIGEL 2.5H and a JAIGEL 3H, in conjugation with UV-600 NEXT UV detector and an FC-3310 fraction collector. Chloroform with 1% EtOH and 0.5% Et_3N was used as mobile phase, with a flow rate of 7.0 mL/min. ESI mass spectra were obtained from the Mass Spectrometry Laboratory at the European Institute of Chemistry and Biology (UMS 3033 - IECB), Pessac, France.

1.1 Synthesis of oligomer 2

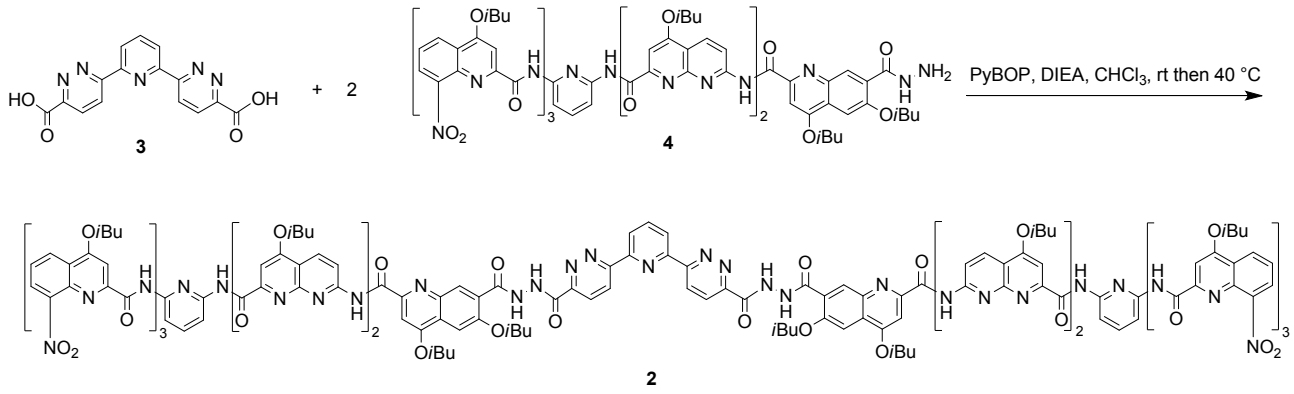

Scheme S1. Synthesis of oligomer **2**.

1.2 Experimental procedures

Oligomer 2: Diacid **3**[1] (17 mg, 0.053 mmol), heptamer amine **4**[2] (180 mg, 0.105 mmol) and PyBOP (275 mg, 0.530 mmol) were dissolved in dry $CHCl_3$ (2 mL). Then, DIEA (0.09 mL, 0.530 mmol) was added at room temperature and the reaction mixture was heated to 40 °C. After two days, the mixture was washed with saturated aqueous. NH_4Cl, followed by saturated aqueous $NaHCO_3$ and finally water. The organic phase was dried on anhydrous $MgSO_4$, filtered and evaporated to dryness. The residue was purified by GPC to yield **2** as a yellow solid (117 mg, 60 %). NMR (300 MHz, CDCl3) δ ppm = 12.04 (s, 2H); 11.73 (s, 2H); 11.51 (s, 2H); 11.12 (s, 2H); 10.64 (s, 2H); 10.47 (s, 2H); 10.35 (s, 2H); 9.88 (s, 2H); 9.08 (d, J = 5.50, 2H); 8.96–8.89 (m, 4H); 8.79 (s, 6H); 8.69 (d, J = 8.18, 2H); 8.49–8.34 (m, 8H); 8.19 (m, 2H); 8.08 (s, 1H); 7.82–7.75 (m, 10H); 7.67 (s, 2H); 7.36–7.24 (m, 7H); 7.15 (s, 2H); 6.98–6.91 (m, 7H); 6.35 (t, J = 7.00, 1H); 4.28–3.65 (m, 24H); 3.31–3.18 (m, 4H); 2.42–2.29 (m, 12H); 1.82 (m, 2H); 1.25–1.15 (m, 70H); 0.90–0.71 (m, 14H); ^{13}C NMR (100 MHz, $CDCl_3$) δ ppm = 163.9, 163.5, 163.4, 163.1, 162.8, 162.1, 161.5, 161.3, 154.7, 154.3, 154.2, 153.6, 152.6, 151.2, 150.9, 149.5, 149.0, 147.5, 145.0, 141.6, 139.8, 138.5, 134.8, 134.0, 127.9, 126.8, 125.9, 125.5, 124.8, 123.9, 123.4, 122.5, 121.1, 117.9, 116.9, 115.3, 114.9, 114.8, 114.2, 109.6, 101.6, 100.8, 99.3, 98.2, 98.0, 97.5, 75.7, 75.3, 74.9, 29.7, 28.3, 28.2, 28.1, 28.0, 19.9, 19.3, 18.8. HRMS (ESI+): *m/z* calcd for $C_{199}H_{197}N_{41}O_{34}$ $[M+2H]^{2+}$ 1854.2585 found 1854.2579.

1-Na^+ complex. Oligomer **1** (2.99 mg, 1.0 μmol) was first dissolved in $CHCl_3$ (300 μL), then a solution (0.005 M) of NaOTf in MeCN (200 μL) was added. The solution was kept stirring for 2h and then the solvent was evaporated to dryness (3.16 mg, quant.). ^{1}H NMR (400 MHz, $CDCl_3/CD_3CN$ 6:4): δ ppm 11.72 (s, 2H), 11.20 (s, 2H), 10.42 (s, 2H), 10.28 (s, 2H), 9.96 (s, 2H), 9.89 (s, 2H), 9.19 (s, 2H), 8.99 (d, J = 7.1 Hz, 2H), 8.77 (d, J = 7.1 Hz, 2H), 8.41 (d, J = 9.5 Hz, 2H), 8.27 – 8.23 (m, 4H), 8.19 – 8.17 (m, 2H), 8.13 (d, J = 7.1 Hz, 2H), 8.05 (d, J = 8.6 Hz, 2H), 7.94 (t, J = 6.2 Hz, 1H), 7.85 (s, 3H), 7.83 (s, 1H), 7.73 (d, J = 7.7 Hz, 2H), 7.32 (d, J = 6.7 Hz, 2H), 7.29 (s, 2H), 7.18 (s, 2H), 7.16 – 7.08 (m, 6H), 7.03 (s, 1H), 7.01 (s, 1H), 6.98 – 6.94 (m, 4H), 6.73 (d, J = 6.7 Hz, 2H), 6.59 (s, 1H), 6.00 (t, J = 6.7 Hz, 2H), 4.62 – 4.58 (m, 1H), 4.56 – 4.52 (m, 2H), 4.41 – 4.37 (m, 2H), 4.30 – 4.27 (m, 2H), 4.21 – 4.17 (m, 2H), 3.73 – 3.64 (m, 4H), 3.40 (d, J = 6.7 Hz, 2H), 3.11 – 3.07 (m, 2H), 2.96 – 2.92 (m, 2H), 2.57 – 2.46 (m, 4H), 2.20 – 2.11 (m, 7H), 1.42 – 1.00 (m, 48H), 0.62 (d, J = 6.9 Hz, 6H), 0.48 (d, J = 6.9 Hz, 6H). HRMS (ESI+): calcd. for $C_{161}H_{152}N_{35}O_{26}Na$ $[M + Na + H]^{2+}$ 1508.0807, found 1508.0211

1-K^+ complex. Oligomer **1** (2.99 mg, 1.0 μmol) was first dissolved in $CHCl_3$ (300 μL), then a solution (0.005 M) of KOTf in MeCN (200 μL) was added. The solution was kept stirring for 2h and then the solvent was evaporated to dryness (3.18 mg, quant.). ^{1}H NMR (400 MHz, $CDCl_3/CD_3CN$ 6:4): δ ppm 11.71 (s, 2H), 11.28 (s, 2H), 10.20 (s, 2H), 10.17 (s, 2H), 9.76 (s, 2H), 9.39 (s, 2H), 8.94 – 8.87 (m, 4H), 8.56 (d, J = 8.9 Hz, 2H), 8.25 – 8.02 (m, 13H), 7.93 (s, 3H), 7.91 (s, 1H), 7.40 (s, 2H), 7.28 (s, 2H), 7.18 – 7.13 (m, 4H), 7.07 (d, J = 7.7 Hz, 2H), 7.02 (d, J = 7.7 Hz, 2H), 6.85 – 6.78 (m, 4H), 6.61 (s, 2H), 6.54 (t, J = 8.1 Hz, 2H), 6.03 (t, J = 8.1 Hz, 2H), 5.91 (s, 2H), 4.61 – 4.58 (m, 1H), 4.52 – 4.48 (m, 2H), 4.32 – 4.25 (m, 4H), 4.20 – 4.17 (m, 2H), 3.75 – 3.66 (m, 4H), 3.43 – 3.35 (m, 4H), 2.97 – 2.93 (m, 2H), 2.56 – 2.43 (m, 5H), 2.32 – 2.28 (m, 2H), 2.23 – 2.14 (m, 4H), 1.38 - 1.05 (m, 48H), 0.59 (d, J = 6.4 Hz, 6H), 0.40 (d, J = 6.3 Hz, 6H). HRMS (ESI+): calcd. for $C_{161}H_{152}N_{35}O_{26}K$ $[M + K + H]^{2+}$ 1515.5659, found 1515.5699.

1-Cu^{2+} complex. Oligomer **1** (2.99 mg, 1.0 μmol) was first dissolved in $CHCl_3$ (300 μL), then a solution (0.005 M) of $Cu(OTf)_2$ in MeCN (200 μL) was added. The solution was kept stirring for 2h and then the solvent was evaporated to dryness (3.35 mg, quant.). HRMS (ESI+): calcd. for $C_{161}H_{152}N_{35}O_{26}Cu$ $[M + Cu + H]^{3+}$ 1018.0309, found 1018.0307.

2-Cu^{2+} complex. Oligomer **2** (3.71 mg, 1.0 μmol) was first dissolved in $CHCl_3$ (300 μL), then a solution (0.005 M) of $Cu(OTf)_2$ in MeCN (200 μL) was added. The solution was kept stirring for 2h and then the solvent was evaporated to dryness (4.07 mg, quant.). HRMS (ESI+): calcd. for $C_{199}H_{197}N_{41}O_{34}Cu$ $[M + Cu]^{2+}$ 1885.2172, found 1885.2344.

2. Methods for NMR, Circular Dichroism and X-ray crystallography

Nuclear Magnetic Resonance. NMR spectra were recorded on two machines: an Avance II NMR spectrometer (Bruker Biospin) with a vertical 7.05T narrow-bore/ultrashield magnet operating at 300 MHz for ^{1}H observation and 75 MHz for ^{13}C observation by means of a 5-mm direct BBO H/X probe with Z gradient capabilities and an Avance 400 NMR spectrometer (Bruker Biospin) with a vertical 9.4T narrow-bore/ultrashield magnet operating at 400 MHz for ^{1}H observation by means of a 5-mm direct QNP $^{1}H/^{13}C/^{31}P/^{19}F$ probe with gradient capabilities. Chemical shifts are reported in parts per million (ppm, δ) with tetramethylsilane as an internal standard. ^{1}H NMR splitting patterns with observed first-order coupling are designated as singlet (s), doublet (d), triplet (t), or quartet (q). Coupling constants (*J*) are reported in hertz. Data processing was performed with Topspin 3.5 software. Samples were not degassed. $CDCl_3$ from Aldrich was used after filtration through an alumina pad.

Circular Dichroism titrations. Titrations were performed in a 2 mm pathlength quartz cuvette at 298.2 ± 0.1 K by adding aliquots of the stock solution of the guest by means of a Hamilton syringe to 0.5 mL solution of the metal complexes. After homogenization and equilibration CD spectra were recorded in the 300–450 nm region on a Jasco J-815 spectropolarimeter. Changes in ellipticity were analysed considering a 1:1 binding model, using the HypSpec program.[3] The errors quoted are the standard deviations of the overall constants given directly by the program for the input data, which include all the wavelengths of each experimental point.

NMR titrations. Titrations were performed in an NMR tube at 298.2 ± 0.1 K by adding aliquots of the stock solution of the guest by means of a Hamilton syringe to 0.500 mL solution of the metal complexes. After homogenization and equilibration NMR spectra were recorded. In the case of the titration of **1-K**$^{+}$ with D/L-**3**, free and bound receptor could be observed simultaneously (slow exchange), thus binding constants K_a were obtained by integration of signals. Values were obtained from several spectra and the results averaged. In the case of the titration of **1-K**$^{+}$ with **4**, fast exchange was observed, thus changes in chemical shift were analysed considering a 1:1 binding model, using the HypNMR program.[4] The errors quoted are the standard deviations of the overall constants given directly by the program for the input data, which include all the wavelengths of each experimental point.

Crystallography. The X-ray diffraction measurements for **1-K**$^{+}$ ⊃ **3** and **1-Cu**$^{2+}$ ⊃ **3** were carried out on a Rigaku FRX rotating anode (2.9 kW) diffractometer at the IECB x-ray facility (UMS 3033 – UMS001). CuKα radiation monochromated with high flux Osmic Varimax mirrors was used for data collections. The x-ray source is equipped with a Dectris Pilatus 200K detector and partial chi goniometer. CrysAlis PRO[5] software was used to process data for **1-K**$^{+}$⊃**3** and **1-Cu**$^{2+}$ ⊃ **3**. Data for **2-Cu**$^{2+}$ ⊃ **5** were measured at the BM30A - FIP (ESRF) beamline using 0.7222 Å wavelength and were processed with the XDS package.[6] **1-K**$^{+}$ ⊃ **3** structure was solved with ShelxD, **1-Cu**$^{2+}$ ⊃ **3** and **2-Cu**$^{2+}$ ⊃ **3** structures with Shelxt.[7] Using Olex2[8] all structures were refined with the ShelXL-2016[7] refinement package using Least Squares minimization.

1-K^{+} ⊃ **3** crystals were X-ray sensitive and two datasets were merged together using XSCALE from XDS package.[7] Before merging three last scans from both datasets were removed. In **2-Cu**$^{2+}$ ⊃ **5** structure anisotropic displacement parameters were used for all atoms but those of disordered isobutoxy side chain. In **1-K**$^{+}$ ⊃ **3** and **1-Cu**$^{2+}$ ⊃ **3** structures only backbones were refined with anisotropic thermal parameters. Position of H atoms of isobutoxy side chains were not determined. For water and guest molecules H atoms were placed on the basis of possible hydrogen bonds. For NH, CH

and CH_2 groups, H atoms were placed at idealized position and were refined in the riding-model approximation, with Uiso(H)=1.2Ueq(CH, CH2, NH) and Uiso(H)=1.5Ueq(OH).

DFIX, AFIX, SAME, SIMU, FLAT, EADP and DELU instructions were employed to model geometry of the molecules and temperature parameters.

In the **1-K^+⊃ 3** and **2-Cu^{2+}⊃ 5** structures some of disordered solvent molecules could not be reliably modeled thus were removed from the model through the use of the SQUEEZE[9] procedure. For search and analysis of solvent accessible voids in the structures default parameters were used: grid 0.20 Å, probe radius 1.2 Å and NStep 6. Calculated total potential solvent accessible void volumes and electron counts per unit cell were 59431 $Å^3$ and 7816, and 2759 $Å^3$ and 860 for **1-K^+⊃ 3** and **2-Cu^{2+}⊃ 5** complexes, respectively.

The final cif files were checked using IUCR's checkcif algorithm. Due to the characteristics of the crystals, i.e. large volume fractions of disordered solvent molecules, weak diffraction intensity, incompleteness of the data and moderate resolution, a number of A-level and B-level alerts remain in the check cif files. These alerts are inherent to the data and refinement procedures and do not reflect errors. Rather, they illustrate the limited practicality of the checkcif tool for medium size molecule crystallography. They are listed below and have been divided into two groups.

Group 1 alerts illustrate weak quality of the data and refinement statistics if compared to that expected for small molecule structures from highly diffracting crystals:

THETM01_ALERT_3_A The value of sine(theta_max)/wavelength is less than 0.550
PLAT023_ALERT_3_A Resolution (too) Low [sin(theta)/Lambda < 0.6]
PLAT029_ALERT_3_A _diffrn_measured_fraction_theta_full value Low
PLAT934_ALERT_3_A Number of (Iobs-Icalc)/SigmaW > 10 Outliers
PLAT023_ALERT_3_B Resolution (too) Low [sin(theta)/Lambda < 0.6]
PLAT082_ALERT_2_B High R1 Value
PLAT084_ALERT_3_B High wR2 Value (i.e. > 0.25)
PLAT220_ALERT_2_B Non-Solvent Resd 1 C Ueq(max)/Ueq(min) Range
PLAT242_ALERT_2_B Low 'MainMol' Ueq as Compared to Neighbors
PLAT340_ALERT_3_B Low Bond Precision on C-C Bonds
PLAT341_ALERT_3_B Low Bond Precision on C-C Bonds
PLAT911_ALERT_3_B Missing FCF Refl Between Thmin & STh/L= 0.590

Group 2 alerts is connected with decision made during refinement and explained below:

PLAT201_ALERT_2_A Isotropic non-H Atoms in Main Residue(s) ..... 104 Report
PLAT201_ALERT_2_B Isotropic non-H Atoms in Main Residue(s) ..... 4 Report
Not all non H-atoms were refined with anisotropic thermal parameters
PLAT306_ALERT_2_B Isolated Oxygen Atom (H-atoms Missing ?)
Unrecognized, isolated electron density peaks were refined as a dummy O atoms.
PLAT602_ALERT_2_A VERY LARGE Solvent Accessible VOID(S) in Structure ! Info
SQUEEZE procedure was used to removed some solvent molecules.
PLAT043_ALERT_1_B Calculated and Reported Mol. Weight Differ by .. 98.87 Check
Not all H atoms were added to the refinement but were added to the SFAC card.

3. Solution studies: Circular Dichroism (CD) and Nuclear Magnetic Resonance (NMR)

3.1 Circular dichroism titrations

Titrations with oligomer **1**

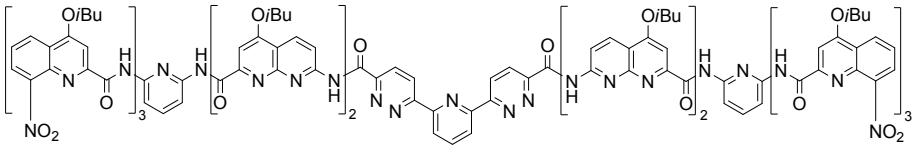

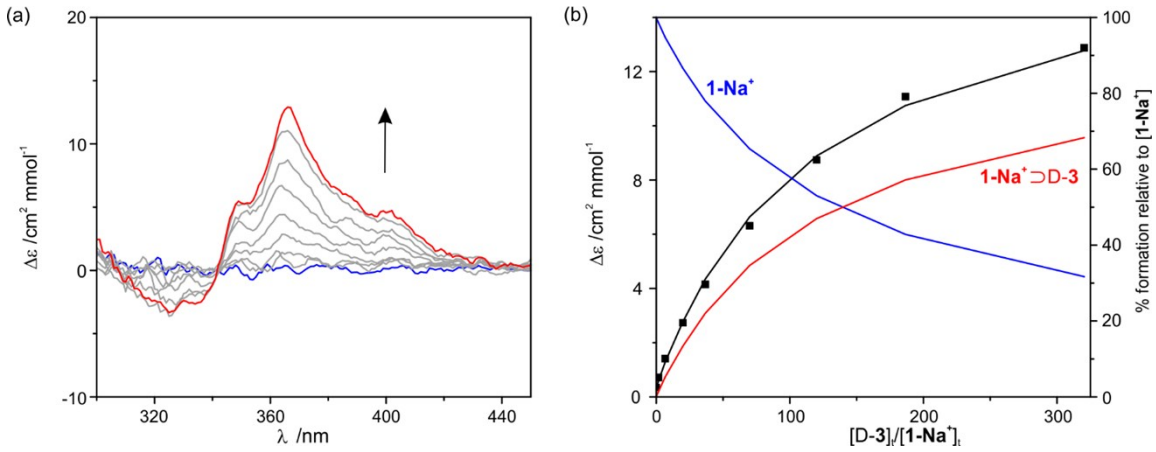

Figure S1. (a) CD spectra recorded at 298 K for the binding study of receptor **1-Na**$^+$ vs. D-**3** in $CHCl_3$/DMSO (9:1 vol/vol). $[\mathbf{1\text{-}Na^+}]_{initial}$ = 0.060 mM, $[\text{D-}\mathbf{3}]_{titrant}$ = 0.01 mM; (b) Experimental and calculated values for the ICD binding study of receptor **1-Na**$^+$ vs. D-**3** in $CHCl_3$/DMSO (9:1 vol/vol) with the corresponding species distribution diagram. Although only Δε values at 366 nm are shown here, all wavelengths in the 300–450 nm region were used for the calculation of the binding constant. K_a = 145 M^{-1}. Limiting Δε (366 nm)= 19 cm^2 $mmol^{-1}$.

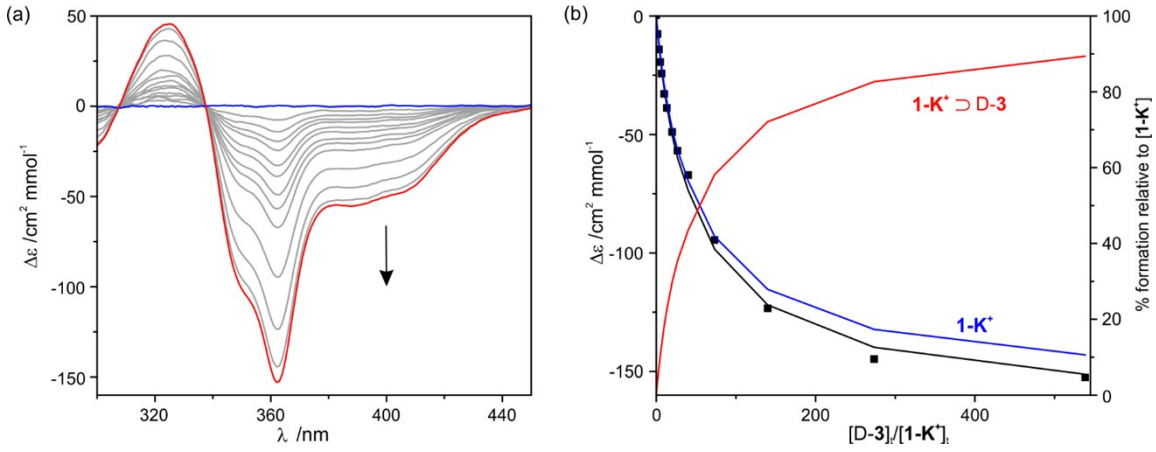

Figure S2. (a) CD spectra recorded at 298 K for the binding study of receptor **1-K**$^+$ vs. D-**3** in $CHCl_3$/DMSO (9:1 vol/vol). $[\mathbf{1\text{-}K^+}]_{initial}$ = 0.060 mM, $[\text{D-}\mathbf{3}]_{titrant}$ = 0.01 mM; (b) Experimental and calculated values for the ICD binding study of receptor **1-K**$^+$ vs. D-**3** in $CHCl_3$/DMSO (9:1 vol/vol) with the corresponding species distribution diagram. Although only Δε values at 362 nm are shown here, all wavelengths in the 300–450 nm region were used for the calculation of the binding constant. K_a = 400 M^{-1}. Limiting Δε (362 nm)= –170 cm^2 $mmol^{-1}$.

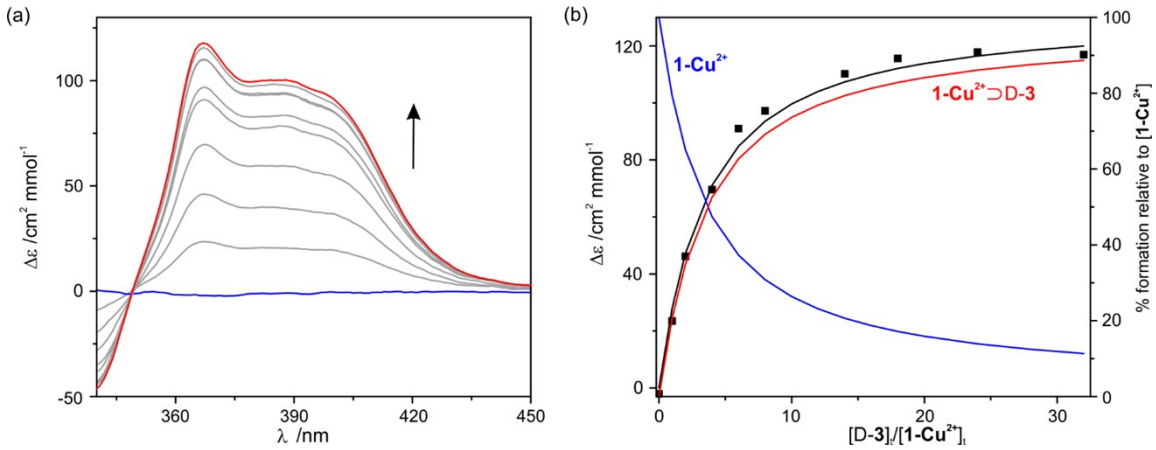

Figure S3. (a) CD spectra recorded at 298 K for the binding study of receptor **1-Cu^{2+}** vs. D-**3** in $CHCl_3$/DMSO (9:1 vol/vol). [**1-Cu^{2+}**]$_{initial}$ = 0.060 mM, [D-**3**]$_{titrant}$ = 0.006 mM; (b) Experimental and calculated values for the ICD binding study of receptor **1-Cu^{2+}** vs. D-**3** in $CHCl_3$/DMSO (9:1 vol/vol) with the corresponding species distribution diagram. Although only Δε values at 367 nm are shown here, all wavelengths in the 340–450 nm region were used for the calculation of the binding constant. K_a = 5500 M^{-1}. Limiting Δε (367 nm) = 137 cm^2 mmol^{-1}.

Titrations with oligomer **2**

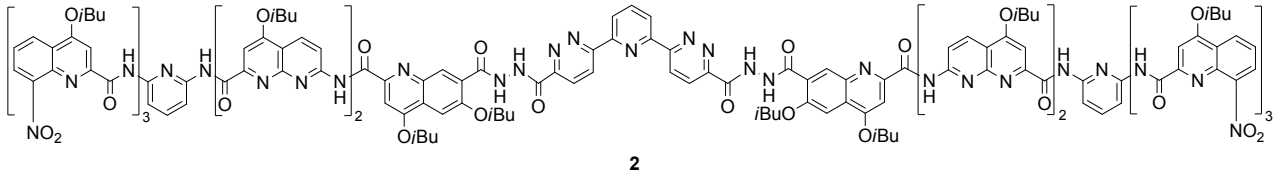

2

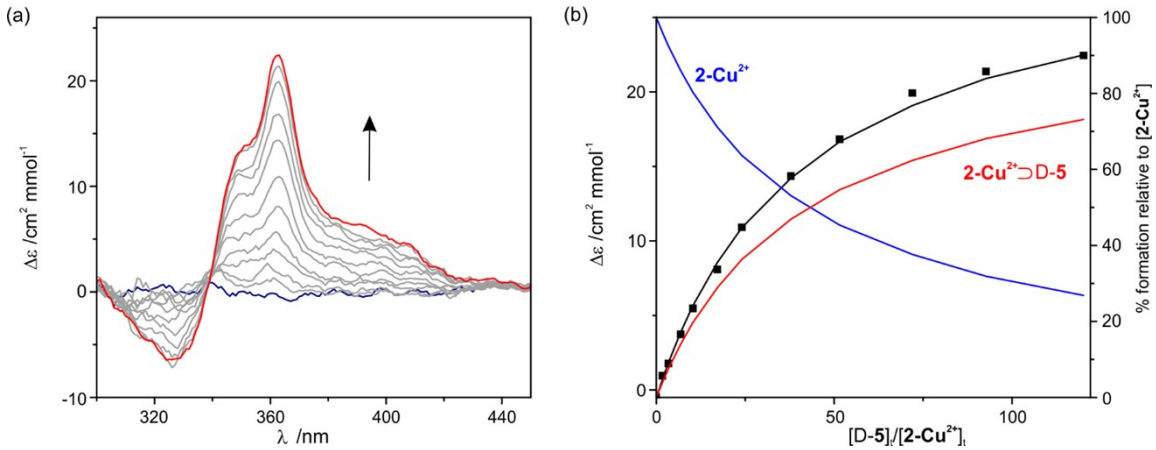

Figure S4. (a) CD spectra recorded at 298 K for the binding study of receptor **2-Cu^{2+}** vs. D-**5** in $CHCl_3$/DMSO (8:2 vol/vol). [**2-Cu^{2+}**]$_{initial}$ = 0.060 mM, [D-**5**]$_{titrant}$ = 0.01 mM; (b) Experimental and calculated values for the ICD binding study of receptor **2-Cu^{2+}** vs. D-**5** in $CHCl_3$/DMSO (8:2 vol/vol) with the corresponding species distribution diagram. Although only Δε values at 363 nm are shown here, all wavelengths in the 300–450 nm region were used for the calculation of the binding constant. K_a = 450 M^{-1}. Limiting Δε (363 nm) = 31 cm^2 mmol^{-1}.

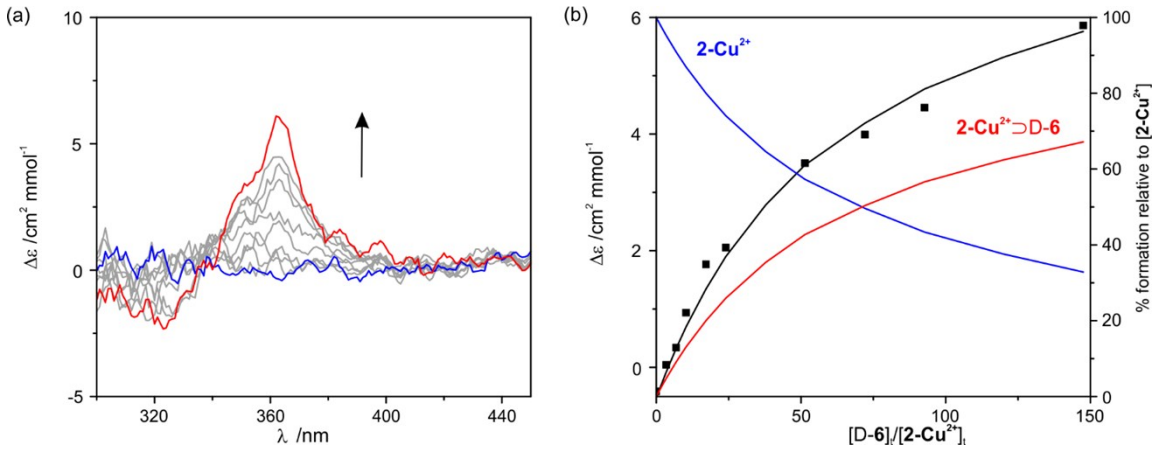

Figure S5. (a) CD spectra recorded at 298 K for the binding study of receptor **2-Cu^{2+}** vs. D-**6** in $CHCl_3$/DMSO (8:2 vol/vol). $[\mathbf{2\text{-}Cu^{2+}}]_{initial}$ = 0.055 mM, $[\text{D-}\mathbf{6}]_{titrant}$ = 0.01 mM; (b) Experimental and calculated values for the ICD binding study of receptor **2-Cu^{2+}** vs. D-**6** in $CHCl_3$/DMSO (8:2 vol/vol) with the corresponding species distribution diagram. Although only Δε values at 364 nm are shown here, all wavelengths in the 300–450 nm region were used for the calculation of the binding constant. K_a = 270 M^{-1}. Limiting Δε (364 nm)= 8.6 cm^2 $mmol^{-1}$.

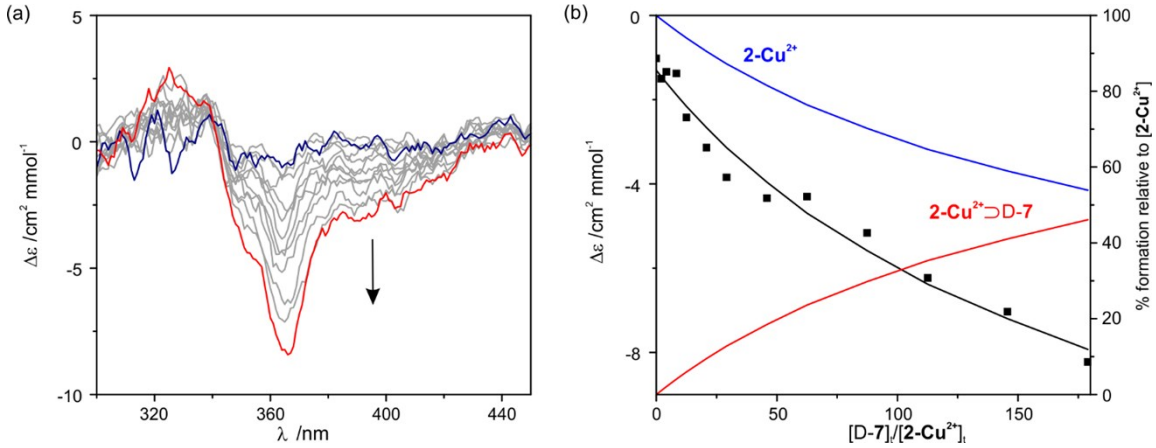

Figure S6. (a) CD spectra recorded at 298 K for the binding study of receptor **2-Cu^{2+}** vs. D-**7** in $CHCl_3$/DMSO (8:2 vol/vol). $[\mathbf{2\text{-}Cu^{2+}}]_{initial}$ = 0.045 mM, $[\text{D-}\mathbf{7}]_{titrant}$ = 0.01 mM; (b) Experimental and calculated values for the ICD binding study of receptor **2-Cu^{2+}** vs. D-**7** in $CHCl_3$/DMSO (8:2 vol/vol) with the corresponding species distribution diagram. Although only Δε values at 364 nm are shown here, all wavelengths in the 300–450 nm region were used for the calculation of the binding constant. K_a = 100 M^{-1}. Limiting Δε (364 nm)= –15.7 cm^2 $mmol^{-1}$.

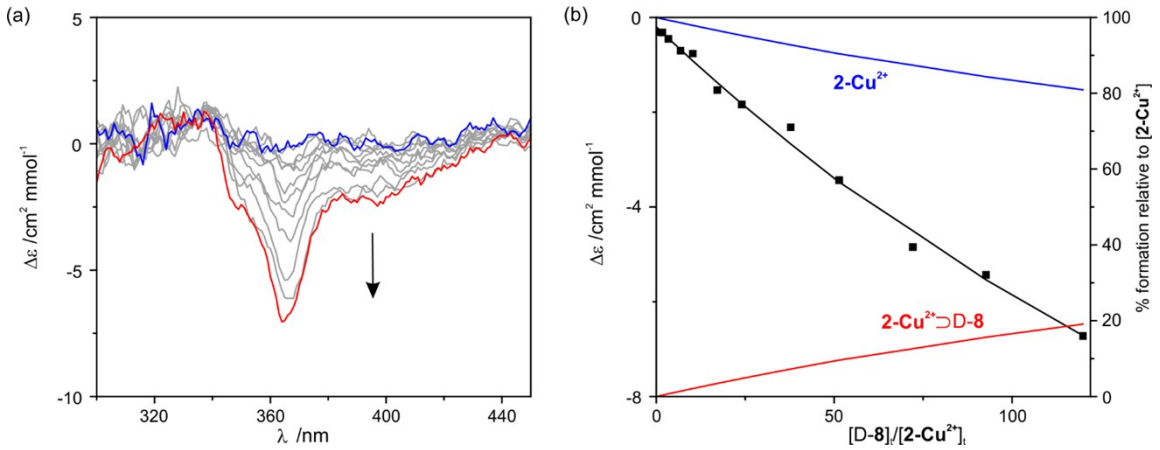

Figure S7. (a) CD spectra recorded at 298 K for the binding study of receptor **2-Cu^{2+}** vs. D-**8** in $CHCl_3$/DMSO (8:2 vol/vol). [**2-Cu^{2+}**]$_{initial}$ = 0.055 mM, [D-**8**]$_{titrant}$ = 0.01 mM; (b) Experimental and calculated values for the ICD binding study of receptor **2-Cu^{2+}** vs. D-**8** in $CHCl_3$/DMSO (8:2 vol/vol) with the corresponding species distribution diagram. Although only Δε values at 364 nm are shown here, all wavelengths in the 300–450 nm region were used for the calculation of the binding constant. K_a = 40 M^{-1}. Limiting Δε (364 nm)= 34 cm^2 mmol^{-1}.

3.2 ^{1}H NMR titrations

Titrations with oligomer **1**

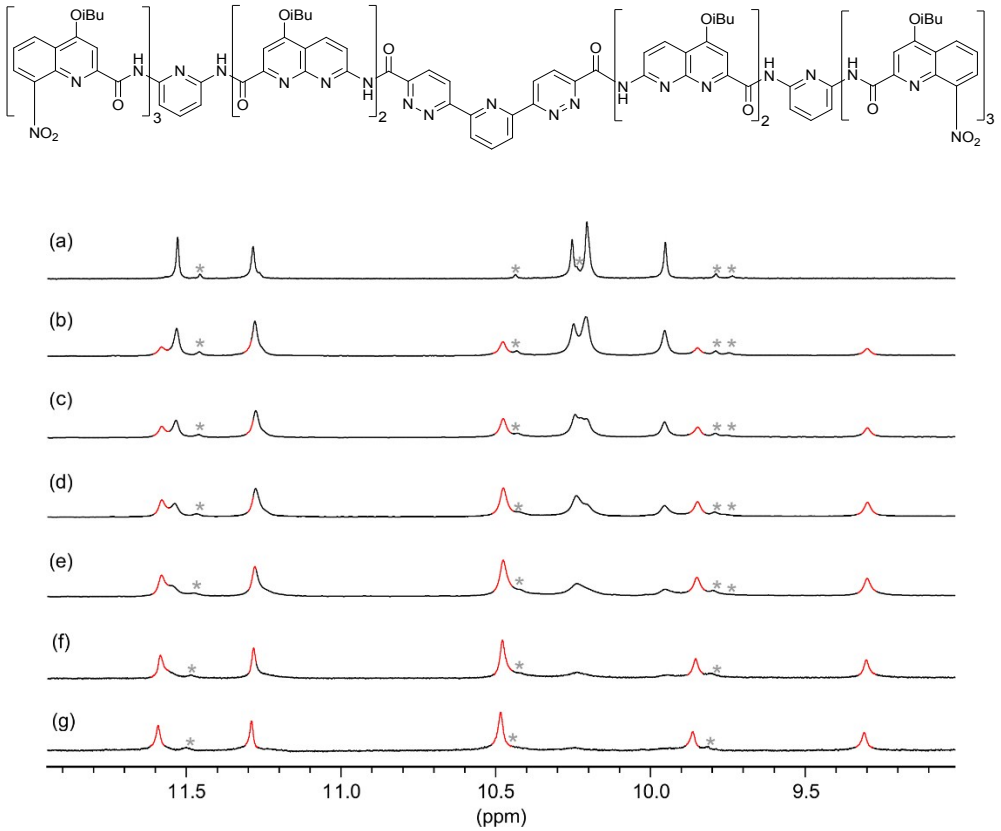

Figure S8. Part of the ^{1}H NMR spectrum (400 MHz) at 298K of receptor **1-K$^+$** (1 mM) in $CDCl_3$/DMSO-d_6 (9:1 vol/vol) showing the amide resonances in the presence of: (a) 0 equiv.; (b) 2 equiv.; (c) 4 equiv.; (d) 8 equiv.; (e) 16 equiv.; (f) 32 equiv.; (g) 64 equiv. of D/L-**3**. Peaks belonging to the **1-K$^+$** ⊃ D/L-**3** complex are marked in red. K_a = 370 M^{-1}. Additional peaks marked as * correspond to a **1-Na$^+$** complex which is present even though no Na^+ was added, as this metal ion is a well-known, ubiquitous contaminant of, for instance, glassware and is strongly bound by **1**.[10]

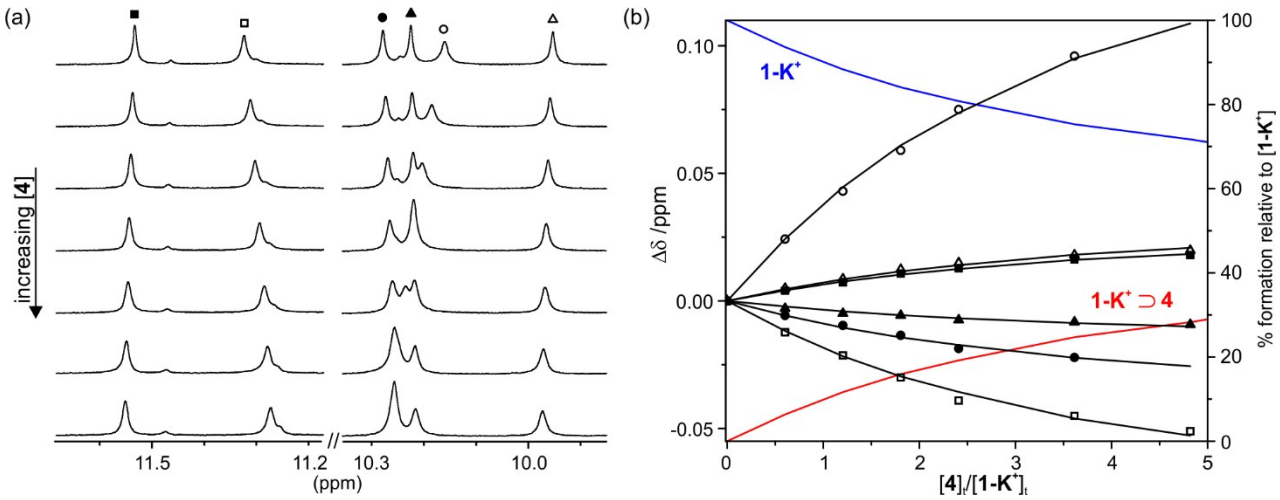

Figure S9. (a) Part of the ^{1}H NMR spectrum (400 MHz) at 298K of receptor **1-K**$^+$ (1 mM) in $CDCl_3$/DMSO-d_6 (9:1 vol/vol) showing the amide resonances in the presence of increasing amounts of **4**. (b) Plot of complexation-induced chemical shifts for the binding study of receptor **1-K**$^+$ vs. **4** in $CHCl_3$/DMSO-d_6 (9:1 vol/vol) with the corresponding species distribution diagram. The symbols are experimental data points; solid lines are best-fit curves obtained through nonlinear regression. $K_a = 150\ M^{-1}$.

4. Solid state X-Ray Crystallography

4.1 X-Ray crystallographic data for the 1-$K^+ \supset$ D/L-3 complex

Table S1. Crystal data and refinement details for the **1-$K^+ \supset$ D/L-3** complex.

Identification code	**1-$K^+ \supset$ 3**
Chemical formula	$2(C_{161}H_{151}N_{35}O_{26}K)\cdot 2(C_4H_{10}O_4)\cdot 2(CF_3O_3S)\cdot C_6H_5Cl\cdot C_2H_3N\cdot 4(CHCl_3)\cdot 2(O)$*
Formula weight	7267.97
Temperature (K)	100(2)
Wavelength (Å)	1.54178 Å
Crystal system	Tetragonal
Space group	$I4_1/a$
Unit cell dimensions (Å, deg)	a=b=65.2962 (7), c=42.3749 (9)
Volume (Å^3)	180669 (5)
Z	16
Density (calculated, Mg mm^{-3})	1.069
Absorption coefficient (mm^{-1})	1.57
Absorption correction	Multi-scan
Index ranges	h = -74→72, k = -73→65, l = -44→47
Completeness to theta = 61.28°	98.5
Reflections collected	286172
Reflections observed [$I > 2\sigma(I)$]	38298
R_{int}	0.074
Data/parameters/restrains	68620/3818/114
Goodness-of-fit on F^2	2.17
Final R indices [$I > 2\sigma(I)$]	R1 = 0.1496, wR2 = 0.3780
R indices (all data)	R1 = 0.2065, wR2 = 0.4041
Largest diff. peak and hole (e Å^{-3})	1.38, -1.04
CCDC 1832021	

*Unrecognized electron density was introduced to the refinement as a dummy oxygen atoms.

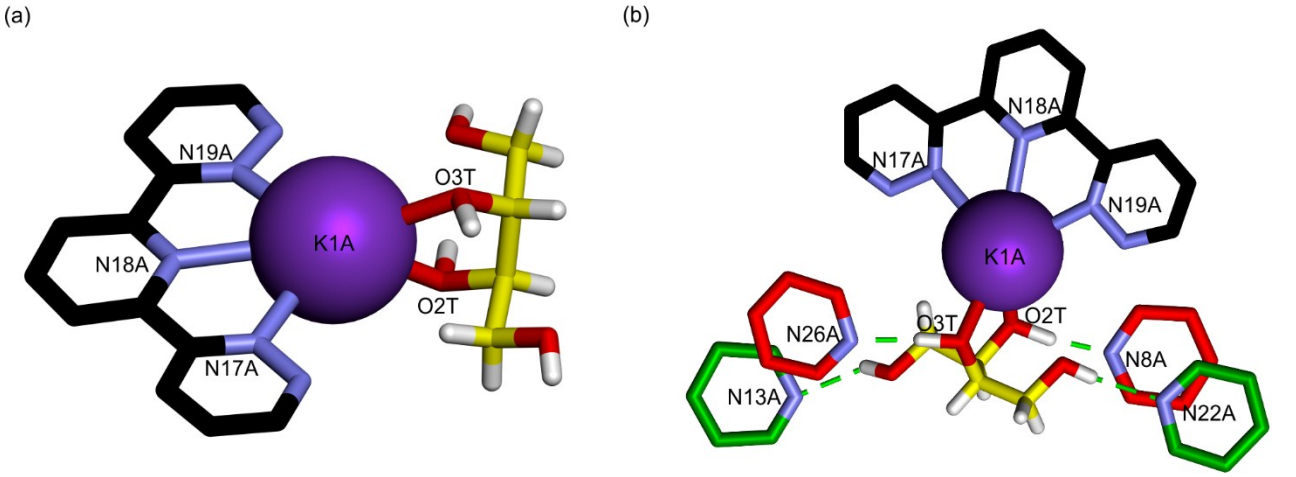

F

igure S10. Detail views of solid-state structure of the **1-$K^+ \supset$ D-3** complex: (a) K first-coordination sphere; (b) Top view showing the heterocycles that interact with the guest molecules. Pyridine monomers are depicted in red, naphthyridine mononers are depicted in green. Potassium atoms are represented in purple balls. Dashed lines indicate hydrogen bonds. Atom numbers are those of the cif file.

Table S2. First-coordination sphere bond lengths (Å) and angles (deg) in the **1-K**$^+$⊃ D-**3** complex.[a]

Bond	**Bond length (Å)**[b]
K1A–O2T	2.680(6)
K1A–O3T	2.826(7)
K1A–N17A	2.943(8)
K1A–N18A	3.150(8)
K1A–N19A	2.789(7)
K2–O6T	2.803(7)
K2–O7T	2.705(7)
K2–N17C	2.791(8)
K2–N18C	3.096(8)
K2–N19C	2.868(10)
	Bond angle (deg)[b]
N19A–K1A–N18A	53.4(2)
N19A–K1A–N17A	105.1(3)
N19A–K1A–O3T	131.9(2)
N19A–K1A–O2T	113.9(2)
N18A–K1A–N17A	52.1(2)
N18A–K1A–O3T	153.7(2)
N18A–K1A–O2T	140.1(2)
N17A–K1A–O3T	117.5(2)
N17A–K1A–O2T	117.5(2)
O3T–K1A–O2T	65.5(2)
N19C–K2–N18C	53.3(3)
N19C–K2–N17C	107.1(3)
N19C–K2–O6T	118.9(3)
N19C–K2–O7T	121.7(3)
N18C–K2–N17C	53.8(2)
N18C–K2–O6T	153.8(2)
N18C–K2–O7T	140.4(2)
N17C–K2–O6T	126.6(2)
N17C–K2–O7T	111.6(2)
O6T–K2–O7T	65.8(2)

[a] Atom numbers are those of the cif file. [b] Values in parenthesis are standard deviations in the last significant figure.

Table S3. O···N distances shorter than 3.25 Åin the **1-K**$^+$⊃D-**3** complex.[a]

	d **(Å)**[b]
O1T···N13A	2.79(1)
O1T···N14A	3.01(1)
O1T'···N14A	3.05(2)
N12A···O1T	3.18(1)
O2T···N8A	2.92(1)
O4T···N22A	2.90(1)
O3T···N28A	2.99(1)
O5T···N14C	2.85(1)
O6T···N8C	2.96(1)
N7C···O6T	3.16(1)
O7T···N28C	2.89(1)
N29C···O7T	3.24(1)
O8T···N23C	2.77(1)
O8T'···N22C	3.02(2)
N24C···O8T	3.17(1)

[a] Atom numbers are those of the cif file. [b] Values in parenthesis are standard deviations in the last significant figure.

4.2 X-Ray crystallographic data for 1-Cu^{2+}⊃ D/L-3 complex

Table S4. Crystal data and refinement details for **1-Cu^{2+}⊃ D/L-3** complex.

Identification code	**1-Cu^{2+}⊃ 3**
Chemical formula	$C_{161}H_{151}O_{26}N_{35}Cu \cdot H_2O \cdot C_4H_{10}O_4 \cdot 2(CSF_3O_3) \cdot 8.07(CHCl_3) \cdot 3.37(O)$ *
Formula weight	4511.05
Temperature (K)	100(2)
Wavelength (Å)	1.54178
Crystal system	Monoclinic
Space group	*C*2/*c*
Unit cell dimensions (Å, deg)	a=49.66 (2), α=90 b=20.107 (7), β=120.16 (1) c=48.86 (2), γ=90
Volume ($Å^3$)	42179 (30)
Z	8
Density (calculated, Mg mm^{-3})	1.421
Absorption coefficient (mm^{-1})	3.86
Absorption correction	Multi-scan
Crystal size (mm)	0.10 × 0.05 × 0.01
Index ranges	h = -52→50, k = -18→21, l = -51→51
Completeness to theta = 55.09°	96.3
Reflections collected	79780
Reflections observed [$I > 2\sigma(I)$]	10516
R_{int}	0.119
Data/parameters/restrains	25634/1993/919
Goodness-of-fit on F^2	1.76
Final R indices [$I > 2\sigma(I)$]	R1 = 0.1625, wR2 = 0.3768
R indices (all data)	R1 = 0.2786, wR2 = 0.4109
Largest diff. peak and hole (e $Å^{-3}$)	1.15, -1.06
CCDC 1832020	

* Unrecognized electron density was introduced to the refinement as a dummy oxygen atoms.

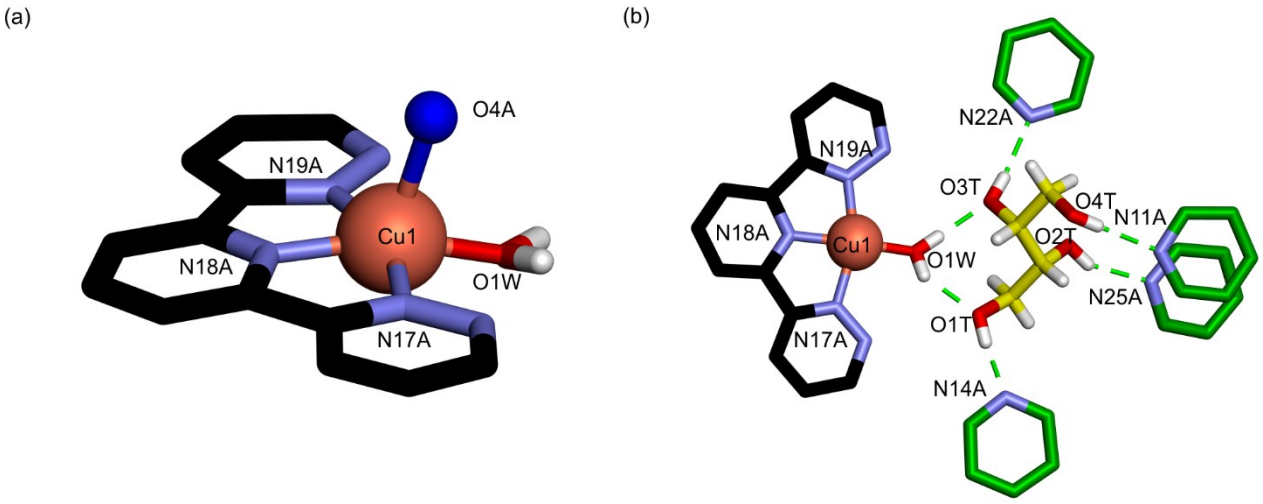

Figure S11. Detail views of solid-state structure of the **1-Cu^{2+}⊃ D-3** complex: (a) Cu first-coordination sphere; (b) Top view showing the heterocycles that interact with the guest molecules. Naphthyridine mononers are depicted in green. Copper atoms are represented in orange balls. Dashed lines indicate hydrogen bonds. Atom numbers are those of the cif file.

Table S5. First-coordination sphere bond lengths (Å) and angles (deg) in the **1-Cu^{2+}** ⊃ D-**3** complex.[a]

Bond	Bond length (Å)[b]
Cu1–O4A	2.180(11)
Cu1–O1W	1.908(10)
Cu1–N17A	1.994(12)
Cu1–N18A	1.934(12)
Cu1–N19A	1.999(13)
	Bond angle (deg)[b]
N17A–Cu1–N19A	157.1(5)
O1W–Cu1–N18A	162.7(5)
N17A–Cu1–O1W	99.5(5)
N17A–Cu1–O4A	89.7(4)
N17A–Cu1–N18A	79.9(6)
O1W–Cu1–O4A	92.3(4)
O1W–Cu1–N19A	99.1(5)
O4A–Cu1–N19A	102.7(4)
O4A–Cu1–N18A	104.9(4)
N19A–Cu1–N18A	78.3(6)

[a] Atom numbers are those of the cif file. [b] Values in parenthesis are standard deviations in the last significant figure.

Table S6. O···N and O···O distances shorter than 3.25 Å between water and D-threitol molecules and capsule heteroatoms in the **1-Cu^{2+}** ⊃ D-**3** complex.[a]

	d **(Å)[b]**
O1W···O1T	2.65(1)
O1W···O3T	2.67(1)
O1T···N14A	2.79(2)
O2T···N25A	2.82(1)
O3T···N22A	2.92(2)
O4T···N11A	2.99(1)
O4T···N10A	3.10(2)
N15A···O1T	3.17(2)
N24A···O2T	3.08(2)
N21A···O3T	3.16(1)

[a] Atom numbers are those of the cif file. [b] Values in parenthesis are standard deviations in the last significant figure.

4.3 X-Ray crystallographic data for 2-Cu^{2+}⊃ D/L-5 complex

Table S7. Crystal data and refinement details for **2-Cu^{2+}⊃ D/L-5** complex.

Identification code	**2-Cu^{2+}⊃ 5**
Chemical formula	$C_{199}H_{197}N_{41}O_{34}Cu \cdot C_6H_{12}O_6 \cdot 3(H_2O) \cdot 2(CF_3O_3S) \cdot CH_3OH \cdot 5.5(CHCl_3)$*
Formula weight	4991.41
Temperature (K)	100(2)
Wavelength (Å)	0.7222 (synchrotron)
Crystal system	Triclinic
Space group	*P*-1
Unit cell dimensions (Å, deg)	a=22.943 (5), α=115.13 (3), b=25.222 (5), β=109.03 (3), c=27.356 (6), γ=92.21 (3),
Volume ($Å^3$)	13255 (6)
Z	2, (Z'=1)
Density (calculated, Mg mm^{-3})	1.251
Absorption coefficient (mm^{-1})	0.34
Absorption correction	none
Crystal size (mm)	0.10 × 0.05 × 0.02
Index ranges	h = -26→26, k = -29→29, l = -31→31
Completeness to theta = 25.22°	92.6
Reflections collected	164227
Reflections observed [$I > 2\sigma(I)$]	34417
R_{int}	0.063
Data/parameters/restrains	42281/2981/77
Goodness-of-fit on F^2	1.019
Final R indices [$I > 2\sigma(I)$]	R1 = 0.0905, wR2 = 0.2660
R indices (all data)	R1 = 0.1037, wR2 = 0.2792
Largest diff. peak and hole (e $Å^{-3}$)	1.32, -1.08

CCDC 1832022

* SQUEEZE procedure was used to remove severely disordered solvent molecules.

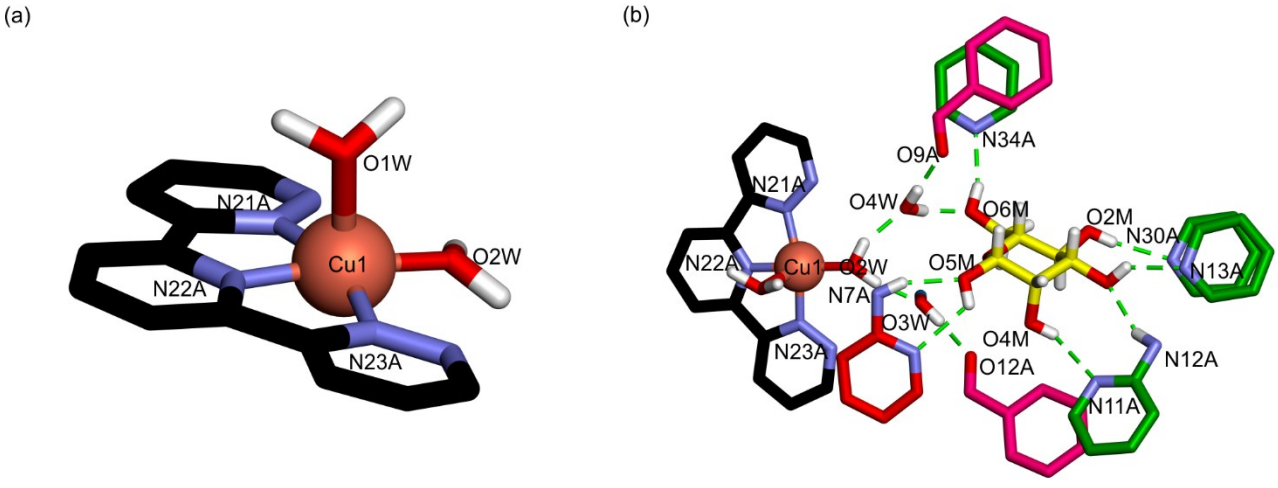

Figure S12. Detail views of solid-state structure of the **2-Cu^{2+}⊃ D-5** complex: (a) Cu first-coordination sphere; (b) Top view showing the heterocycles that interact with the guest molecules. Pyridine, naphthyridine and hydrazine mononers are depicted in red, green and magenta, respectively. Copper atoms are represented in orange balls. Dashed lines indicate hydrogen bonds. Atom numbers are those of the cif file.

Table S8. First-coordination sphere bond lengths (Å) and angles (deg) in the **2-Cu^{2+}** ⊃ D-**5** complex.[a]

Bond	**Bond length (Å)**[b]
Cu1–O1W	2.251(3)
Cu1–O2W	1.895(3)
Cu1–N21A	1.961(4)
Cu1–N22A	1.930(4)
Cu1–N23A	1.982(4)
	Bond angle (deg)[b]
N22A–Cu1–O2W	174.0(2)
N21A–Cu1–N23A	158.0(2)
N21A–Cu1–N22A	80.1(2)
N21A–Cu1–O2W	100.1(2)
N21A–Cu1–O1W	101.0(2)
N22A–Cu1–N23A	80.5(2)
N22A–Cu1–O1W	83.3(1)
N23A–Cu1–O2W	97.4(2)
N23A–Cu1–O1W	86.8(2)
O2W–Cu1–O1W	102.2(1)

[a] Atom numbers are those of the cif file. [b] Values in parenthesis are standard deviations in the last significant figure.

Table S9. O···N and O···O distances shorter than 3.25 Å between water and D-mannose molecules and capsule heteroatoms in the **2-Cu^{2+}** ⊃ D-**5** complex.[a]

	***d* (Å)**[b]
O1W···O5A	2.656(5)
O2W···O4W	2.595(4)
O2W···O3W	2.584(6)
O3W···O12A	2.603(5)
N25A···O3W	3.085(6)
O4W···O9A	2.666(5)
O4W···O6M	2.743(5)
N19A···O4W	2.853(5)
O6M···N34A	2.814(5)
N35A···O6M	2.997(5)
O2M···N30A	2.929(5)
O3M···N13A	2.863(5)
N12A···O3M	3.035(5)
O4M···N11A	3.170(5)
N7A···O5M	2.886(5)
O5M···N8A	2.911(6)

[a] Atom numbers are those of the cif file. [b] Values in parenthesis are standard deviations in the last significant figure.

5. ^{1}H NMR and ^{13}C NMR spectra of new synthetic compounds

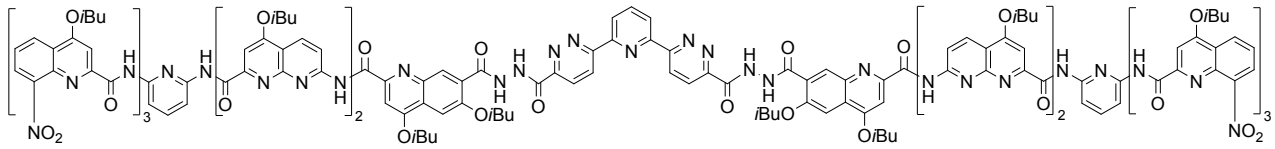

2

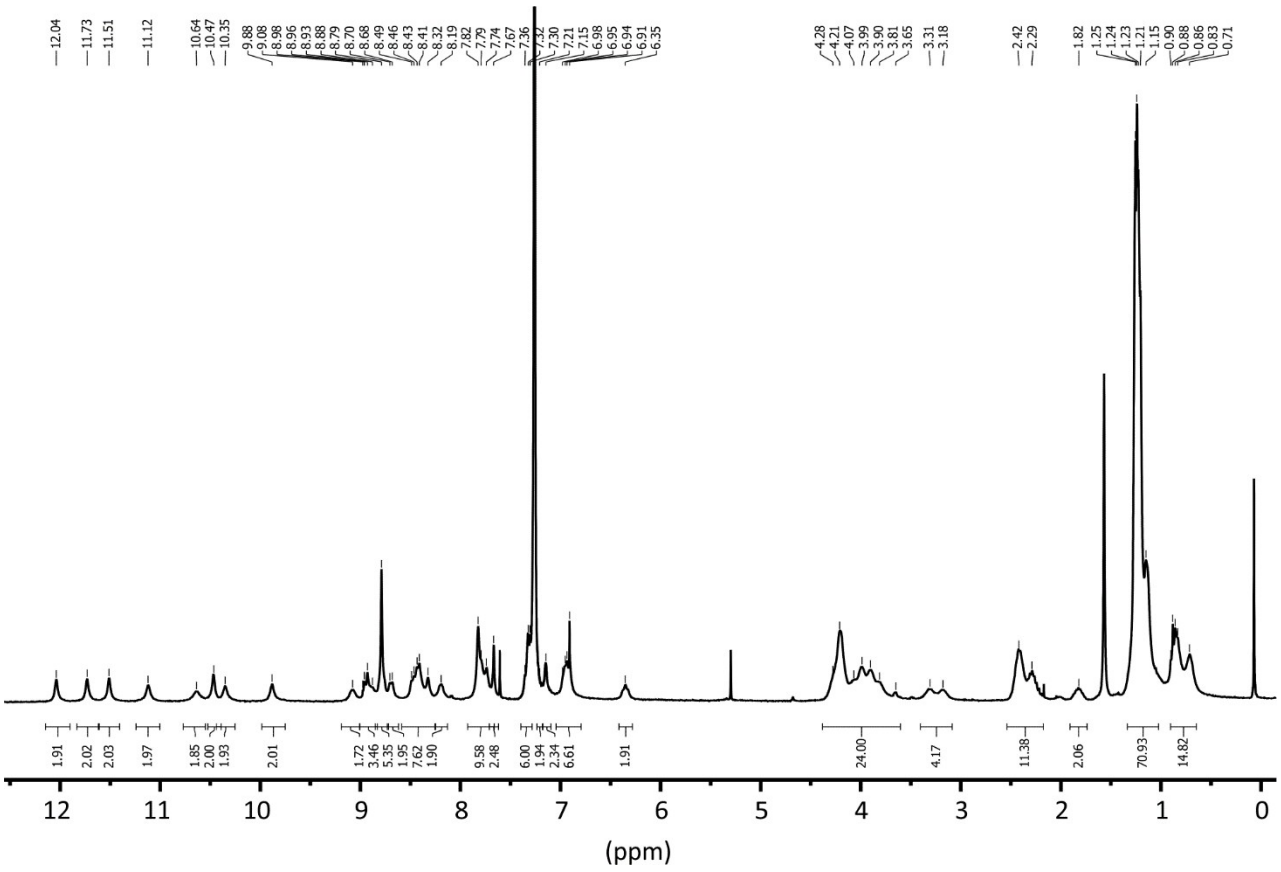

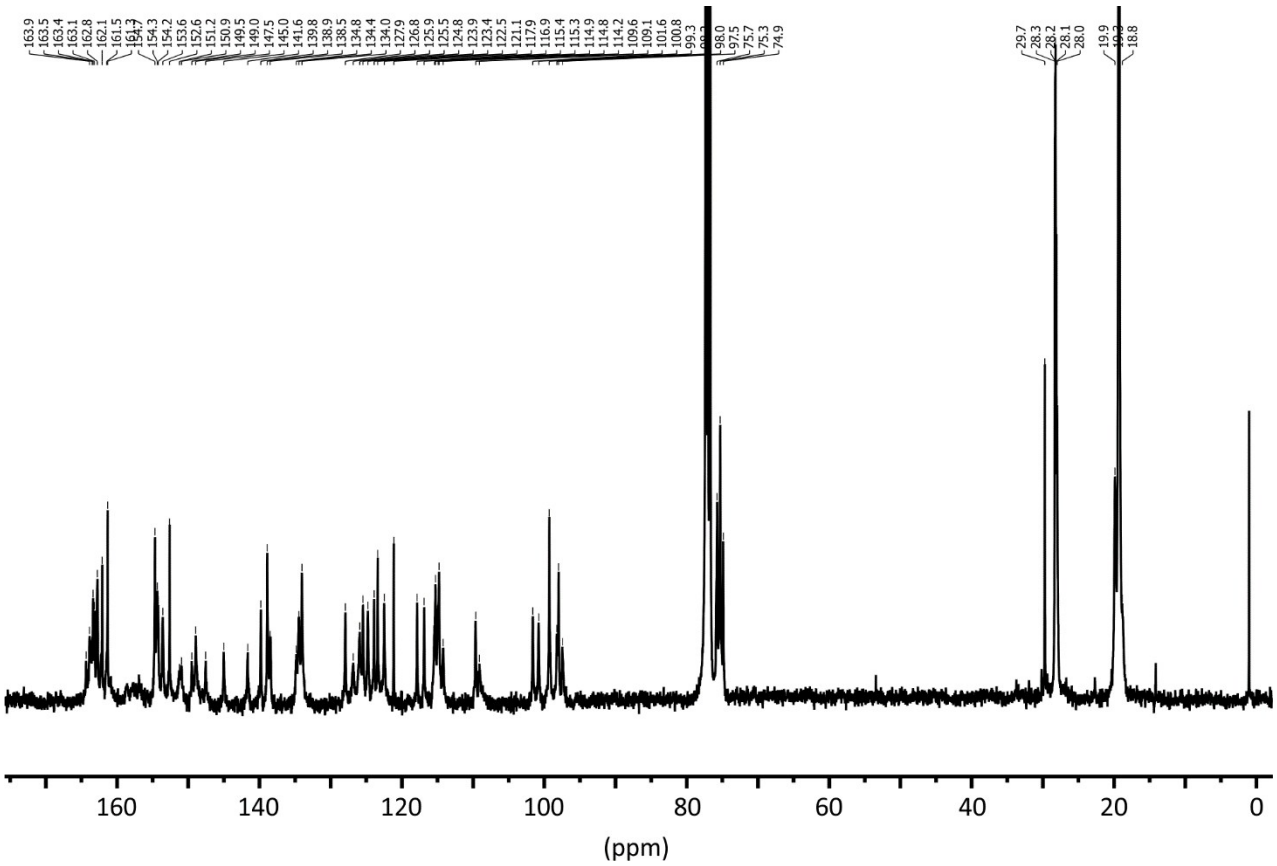
163.9
163.5
163.4
163.1
162.8
162.1
161.5
154.3
154.2
153.6
152.6
151.2
150.9
149.5
149.0
147.5
145.0
141.6
139.8
138.9
138.5
134.8
134.4
134.0
127.9
126.8
125.9
125.5
124.8
123.9
123.4
122.5
121.1
117.9
116.9
115.4
115.3
114.9
114.8
114.2
109.6
109.1
101.6
100.8
99.3
98.0
97.5
75.7
75.3
74.9
29.7
28.3
28.2
28.1
28.0
19.9
18.8
160
140
120
100
80
60
40
20
0
(ppm)

6. References

1 M. Horeau, G. Lautrette, B. Wicher, V. Blot, J. Lebreton, M. Pipelier, D. Dubreuil, Y. Ferrand and Ivan Huc, *Angew. Chem. Int. Ed.*, 2017, **56**, 1.

2 Y. Ferrand, N. Chandramouli, A. M. Kendhale, C. Aube, B. Kauffmann, A. Grélard, M. Laguerre, D. Dubreuil and I. Huc, *J. Am. Chem. Soc.*, 2012, **134**, 11282.

3 P. Gans, A. Sabatini and A. Vacca, *Ann. Chim*.1999, **89**, 45.

4 (a) C. Frassineti, S. Ghelli, P. Gans, A. Sabatini, M. S. Moruzzi and A. Vacca, *Anal. Biochem.*, 1995, **231**, 374. (b) C. Frassineti, L. Alderighi, P. Gans, A. Sabatini and A. Vacca, S. Ghelli, *Anal. Bioanal. Chem.*, 2003, **376**, 1041.

5 *CrysAlis PRO Software*; Agilent Technologies: Yarton, Oxfordshire, England, **2014**.

6 W. Kabsch, *Acta Cryst.*, 2010, **D66**, 125.

7 G. M. Sheldrick, *Acta Cryst.*, 2015, **C71**, 3.

8 O. V. Dolomanov, L. J. Bourhis R. J. Gildea, J. A. K. Howard and H. Puschmann, *J. Appl. Cryst.*, 2009, **42**, 339.

9 A. L. Spek, *Acta. Cryst.*, 2015, **C71**, 9.

10 P. Mateus, B. Wicher, Y. Ferrand and I. Huc, *Chem. Commun.*, 2017, **53**, 9300